Control of a particular Micro-Macro positioning system applied to cell Micromanipulation.

Michaël Gauthier, Emmanuel Piat

▶ **To cite this version:**

Michaël Gauthier, Emmanuel Piat. Control of a particular Micro-Macro positioning system applied to cell Micromanipulation.. IEEE Transactions on Automation Science and Engineering, 2006, 3 (3), pp.264-271. 10.1109/TASE.2005.861398 . hal-00264443

HAL Id: hal-00264443
https://hal.science/hal-00264443

Submitted on 17 Mar 2008

HAL is a multi-disciplinary open access archive for the deposit and dissemination of scientific research documents, whether they are published or not. The documents may come from teaching and research institutions in France or abroad, or from public or private research centers.

L'archive ouverte pluridisciplinaire **HAL**, est destinée au dépôt et à la diffusion de documents scientifiques de niveau recherche, publiés ou non, émanant des établissements d'enseignement et de recherche français ou étrangers, des laboratoires publics ou privés.

Control of a particular micro-macro positioning system applied to cell micromanipulation

Michaël Gauthier (corresponding author) and Emmanuel Piat
Laboratoire d'Automatique de Besançon: LAB UMR CNRS 6596
24, rue Alain Savary - 25000 Besançon - France
Tel: +33 (0) 381 402 810 - Fax: +33 (0) 381 402 809
Website: http://www.lab.cnrs.fr, E-mail: gauthier@ens2m.fr

***Abstract*— Biological research requires new tools for cell micromanipulations. Currently, biological cell sizes range from a few to hundreds of micrometers, their manipulation therefore belonging to the field of microrobotics. This paper presents a new wireless micromanipulation system which allows cells placed in a droplet of liquid to be pushed on a glass slide. The cell micropusher is a ferromagnetic object which follows the movement of a permanent magnet located under the glass slide. It has been proved in previous works that two kinds of micropusher movements can induce a movement of the pushed object: turning the micropusher around the contact point (rotation), or moving the micropusher in translation. Rotation allows an object to be placed with a precision below 1 μm ,but acts within a narrow range. Translation allows placement of an object with lower accuracy, but within a wide range. We propose a specific coarse-fine control strategy to push an object, with good precision, within a wide range. Furthermore, experimentation on polystyrene balls of 50 μm in diameter, and immature human oocytes of 150 μm in diameter are presented.**

***Index Terms*— microrobotics, micromanipulation, coarse-fine control, biological object, magnetic.**

I. Introduction

At present, there is great interest in automation of cell micromoving, testing, characterization and treatment [1-6].In fact, biological micromanipulations are currently performed manually and efficiency is relatively low. Automation and development of new cell characterisations may lead to the proposal of new automatic processes with higher efficiency. This study focuses on the In Vitro Fertilisation (IVF) process, whose efficiency is currently only about 30%.

Our goal is to build an automatic In Vitro Fertilisation device composed of standard modules such as a cumulus removal module, and an oocyte stiffness sensor module or an injection module. A cell transport system to supply all the modules is also needed. Two modules are presently under development: the oocyte stiffness sensor module [7, 8] and the transport system described here. This work is under way in collaboration with physicians: Prof. C. Roux of the Genetic and Reproduction research team of the University of Franche-Comté, France.

Conventional glass micropipette is a competitive tool for the manipulation of oocytes. However, complex trajectories, complex shunting, or manipulation of an oocyte placed behind another oocyte cannot be performed with conventional micropipettes. Consequently, we propose a new technology allowing complex oocyte trajectories.

The cell transport module can push an oocyte placed in a droplet of a biological liquid on a glass slide with a ferromagnetic microscopic pusher ($200 \times 200 \times 20$ μm^3). This pusher follows the movement of a permanent magnet located beneath the glass slide (figure 1(a)). Two types of pusher movement can generate a object motion by pushing:

- contact point movement between the glass slide and the pusher (figure 1(b)),
- pusher rotation around the contact point (figure 1(c)).

The first type induces large movements but is disturbed by friction effects, whereas the second induces fine movements without friction disturbances. Consequently the pusher may be compared to a micro-macro positioning system. As both micro and macro-movement depend on the same input (magnet position), classical micro-macro positioning strategies are not usable. This article therefore proposes a specific micro-macro positioning strategy for control of the pushed object's position.

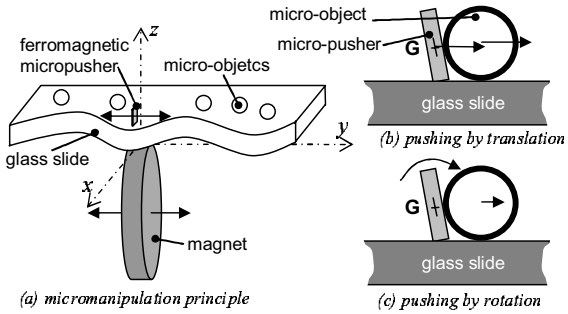

Fig. 1. Micromanipulation principles

Previous studies of the micromanipulation device were undertaken in [9, 10]. Modelling of the pusher behaviour in function of both friction properties and magnetic properties were studied in [10]. This article focuses on the strategy used for automatic control of the position of the manipulated object. Since a presentation of pusher behaviour is necessary to understand control strategy, Part III is devoted to a

summary of the model presented in [10].

In Part II the micromanipulation experimental device is presented. Part III describes micropusher behaviour in function of magnet position, and summarises the model presented in [10]. Part IV presents control strategy and the controller. Experimental micromanipulations and control tests are presented in Part V.

II. Experimental Micromanipulation Device

Magnetic energy is of great interest in micromanipulation [11-20], especially in cell manipulation. Obviously, the magnetic field easily crosses glass slides used in biological manipulations [21]. By this way, an external magnetic field is thus able to control the position of a submerged micro-object without mechanical contact with the external environment. The use of wireless energy avoids cross contamination between external and biological media. Furthermore, cells are generally neither magnetic nor ferromagnetic, so the magnetic field does not disturb the cell positions. Finally, the magnetic field disturbs neither the movement nor the chemical properties [21] of the aqueous media. Given these advantages, we chose to use magnetic energy to build the cell micromanipulator.

The micro-pusher is made of electroplated nickel [9]. At the present time, the micro-pusher is not biocompatible and we are working on two solutions for the problem: encapsulation of the current micropusher in a biocompatible material, and the use of magnetic biocompatible materials.

A photo of the experimental device is presented in figure 2. The magnet is a cylindrical magnet of axis $\overrightarrow{y}$ with vertical magnetization, a diameter of $5\,mm$ and a thickness of $1\,mm$.

This principle allows control the position of the micropusher in two directions, however the modelling of the device, and the control strategy are presently undertaken in a single direction $\overrightarrow{y}$. In this article, we present the strategy used to control the position of the micropusher in this direction. The magnet moves along the axis $\overrightarrow{y}$ by means of a micro-actuator (see figure 2).

The voltage input of the micro-actuator is controlled by computer (see figure 3), and the magnet position is measured by a laser position sensor. The work place image, determined by a CCD camera, allows measurement of both the micropusher and cell positions. Micropusher contact point position and centre of gravity is measured via a binary image furnished by the CCD Camera.

III. Micropusher behaviour

This section summarises pusher behaviour (orientation and translation) so as to introduce a comparison between our device and a standard micro-macropositioning system. A control strategy outline is presented, and detailed in the next section.

To present micropusher behaviour, some notations are necessary: point O is the center of the top of the cylindrical magnet defined in figure 4. Points G and I respectively designate the centre of gravity of the micropusher and the contact point between the micropusher and the glass slide. Micropusher height is noted h.

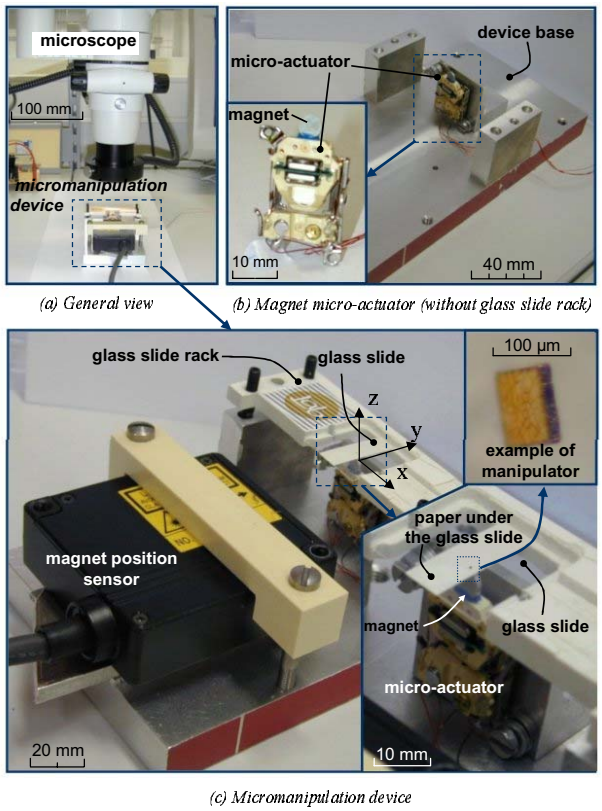

(a) General view (b) Magnet micro-actuator (without glass slide rack)

(c) Micromanipulation device

Fig. 2. Experimental device.

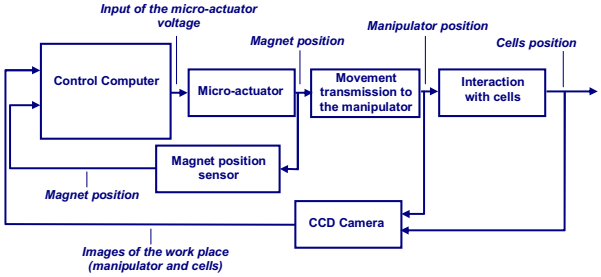

Fig. 3. Information transmission in the experimental device.

If we consider only one axis of movement (direction $\overrightarrow{y}$ in figure 2), two parameters define the position of the micropusher:

- position y_I of the contact point I, and
- micropusher orientation defined by $d = y_G - y_I$ (figure 4(a)).

A. Micropusher Orientation

Pusher orientation is given by the equilibrium between magnetic force torque and magnetic torque. Magnetic force torque aims to put the pusher on the glass slide, while magnetic torque aims to align pusher on the magnetic field lines. In microscale, magnetic torque is greater than magnetic force torque, and the pusher remains aligned on the magnetic field line, the latter fact proved in [10].

Micropusher orientations are presented in figure 4(b). It was also proved that the micropusher orientation d is proportional to the difference $(y_G - y_O)$:

$$d = y_G - y_I = K(y_G - y_O) \quad (1)$$

with: K function of the micropusher shape

eg: $K = 0.16$ with $h = 200\,\mu m$ (2)

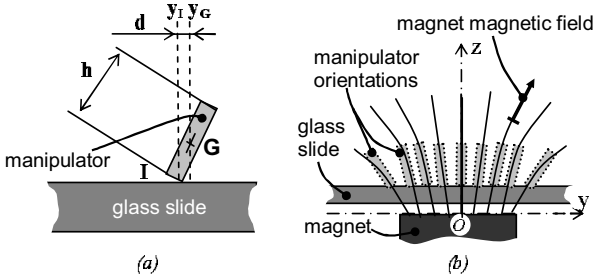

Fig. 4. Micropusher orientation and definition of parameter d.

B. Translation behaviour

Contact point behaviour is defined by Coulomb's friction laws. A synthesis of this behaviour is presented in figure 5. In cases (a) and (c), the micropusher (y_G) moves by small fits and starts in the same direction as the magnet (y_O). Fits and starts are induced by the friction on the glass slide, a phenomenon called *stick-slip*. In these cases, contact point I moves and micropusher orientation d remains constant. In cases (b) and (d), the point I is fixed, the micropusher remains aligned on the magnetic field lines. Micropusher orientation changes, thus centre of gravity position y_G changes also. Therefore, point G moves in the opposite direction of the magnet O. When the magnet goes forward and backward, the position G describes the hysteresis cycle presented in the center of figure 5.

Complete modelling of pusher behaviour is presented in [10]. To simplify the control strategy presentation, stick slip effect is not take into account in the following explanations, though the control strategy experimentations presented are carried out on a simulator which does takes this effect into account.

The contact point position y_I is a "backlash function" (or "dead-zone function") in function of the magnet position y_O (figure 5). Parameter L_c is defined so that $(1-K)L_c$ represents the play found in this backlash function. Thus:

$$-\frac{(1-K)L_c}{2} < y_I - y_O < \frac{(1-K)L_c}{2} \quad (3)$$

$$\text{or: } -\frac{L_c}{2} < y_G - y_O < \frac{L_c}{2} \quad \text{from (1)} \quad (4)$$

L_c represents the maximum amplitude of the difference $(y_G - y_O)$ and depends on the friction coefficient and magnetic forces. An example of the measured value of L_c is presented in [10]:

$$L_c = 680\,\mu m \quad (5)$$

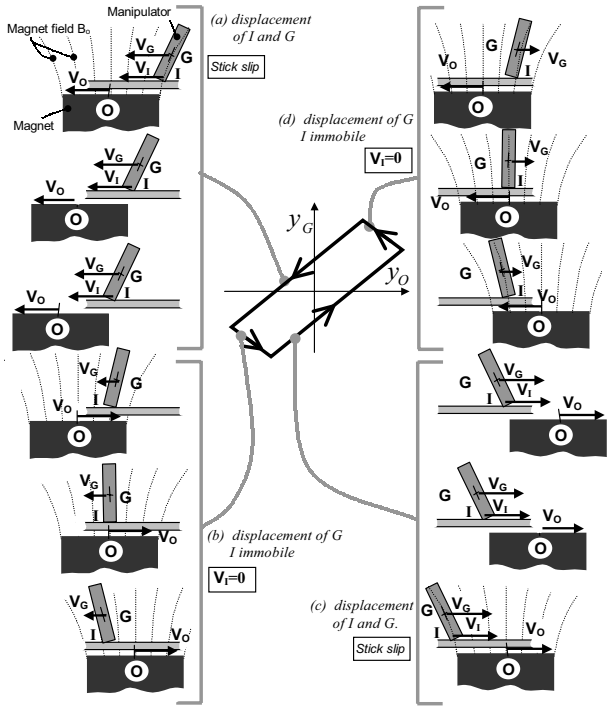

Fig. 5. Micropusher behaviour description: (a) Points I and G move by small fits and starts to the left; (b) half-turn of the magnet, point I remains fixed, micropusher orientation changes and point G moves to the left again; (c) the micropusher follows magnet movement to the right; (d) I is fixed, G moves to the right.

Furthermore:

$$d = y_G - y_I = K(y_G - y_O) \quad \text{from (1)}$$

$$\text{so: } d = \frac{K}{1-K}(y_I - y_O) \quad (6)$$

Moreover d satisfies:

$$-d_M \leq d \leq d_M \quad \text{from (3)} \quad (7)$$

$$\text{with: } d_M = K.\frac{L_c}{2} \quad (8)$$

Briefly, the position of the micropusher centre of gravity y_G is the sum of d and y_I (see equation (1)). Contact point position y_I is a backlash function of the magnet position y_O, and pusher orientation d depends on y_I and y_O (see equation (6)). The block function defined in figure 6 is obtained and noted *PUSHER1D*.

C. Micro-macro positioning system

The micropusher has two types of behaviour (figure 6):

- contact point y_I is fixed and the movement of the magnet y_O modifies orientation of micropusher d;
- contact point y_I moves in the same direction as magnet y_O, distance $(y_I - y_O)$ is constant and orientation d is constant $(d = \pm d_M)$.

The centre of gravity movement induced by the modification of the micropusher orientation d is noted "MICRO movement". Likewise, the movement of the

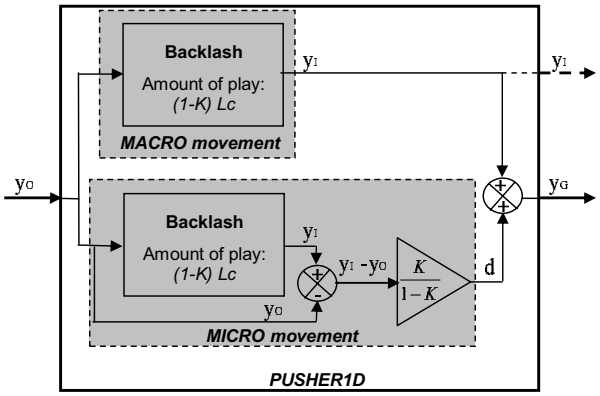

Fig. 6. The *PUSHER1D* block function: a micro-macropositionning system.

micropusher centre of gravity induced by the contact point movement is noted "MACRO movement". MICRO and MACRO movements cannot both occur at the same time. The properties of both behaviours are presented in table I. In fact, MICRO movement is not disturbed by the stick-slip effect and so can induce a precise movement but only within a narrow range. Contrary to MICRO movement, MACRO movement is disturbed by the stick slip effect, but acts within a wide range.

Type	MACRO	MICRO
$\mathbf{y_I(t)} =$	$y_O(t) + cnt$	cnt
$\mathbf{d(t)} =$	$cnt\ (\pm d_M)$	$\frac{-K}{1-K} y_O(t) + cnt$
$\mathbf{y_G(t)} =$	$y_O(t) + cnt$	$\frac{-K}{1-K} y_O(t) + cnt$
Stick slip	yes	no

cnt: constant

TABLE I
PROPERTIES OF BOTH MACRO AND MICRO BEHAVIOURS

Our system is comparable to a micro-macro positioning system (figure 7(a)). The greatest difference between a conventional micro-macro positioning system (described in figure 7(b)), and this system (described in figures 6 and 7(a)), is that our device has only one input for both behaviours (MICRO and MACRO). Control strategies used in conventional micro-macro positioning systems (see example in [23]) are not usable.

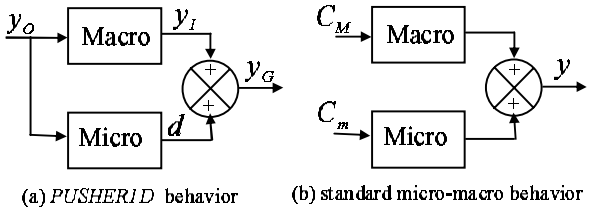

Fig. 7. (a) *PUSHER1D* micro-macro positioning system; (b) Standard micro-macro positioning system.

D. Control strategy

The control strategy goal is to control the position of the pushed object. We consider that the diameter of the object is the height of the manipulator. If G_c and G are defined as the centre of gravity of the cell and the manipulator respectively, then the distance G_cG is:

$$G_cG \simeq \frac{h}{2}.\left(1+\frac{1}{2}\left(\frac{d}{h}\right)^2\right) \simeq \frac{h}{2} \tag{9}$$

$$\text{because: } \left(\frac{d}{h}\right)^2 < \left(\frac{K\,L_c}{2h}\right)^2 \quad \text{from (7)} \tag{10}$$

$$< 9\,10^{-3} \quad \text{from (5,2)} \tag{11}$$

We assume in this article that the relative position of G and G_c is a constant ($\frac{h}{2}$). Therefore the relative position between the pusher centre of gravity reference y_C and the object reference is a constant also (figure 8(a)). Consequently, it can be considered that object position control is equivalent to micropusher gravity centre control. Thus, only the position control of the pusher gravity centre is studied.

The specific control strategy is described briefly in figure 8. The objective is to push an object from the initial position (figure 8(a)) to the reference position y_C (figure 8(f)). We propose two steps:

- a MACRO movement (figure 8(b-c)), then
- a MICRO movement (figure 8(d-e)).

In the next section, the control strategy used to induce the behaviour described in figure 8 is described.

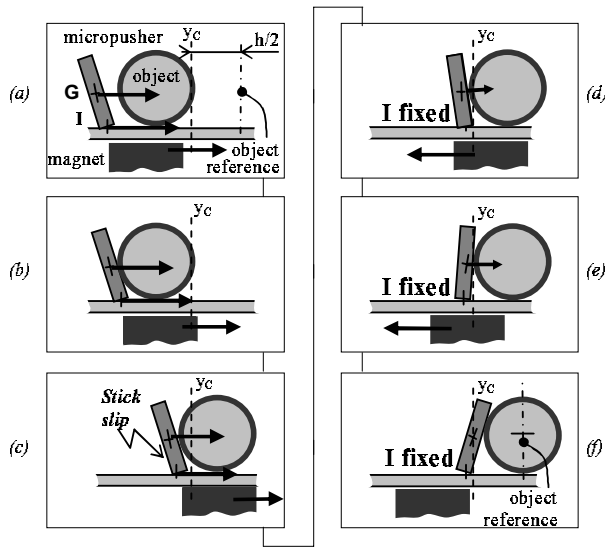

Fig. 8. Control strategy.

IV. POSITION CONTROL

This section is devoted to the description of the position controller, which is comprised of a supervisor and three specialized PI controllers.

A. Supervisor description

The *PUSHER1D* block function defines the behaviour of y_G in function of y_O. This function switches between two linear behaviours (MICRO and MACRO). We chose to build two specific controllers for each behaviour (MICRO and MACRO). The objective of the supervisor is to choose the controller according to both reference position and micropusher position and orientation.

The controllers used for MICRO and MACRO movements are noted "fine controller" and "coarse controller" respectively. The next sections present the specificities of these two kinds of controllers.

1) Fine control: we define the condition for fine controller use by means of the "approach zone" noted Z_a. The center of Z_a is the reference position y_C and Z_a satisfies (figure 9):

$$y_I \in Z_a \Rightarrow y_C \text{ is accessible by } G \text{ in MICRO movement} \tag{12}$$

Parameter d_M is defined as the maximal value of orientation d (introduced in equation (8)), so:

$$y_C \text{ is accessible in MICRO movement} \Leftrightarrow y_I \in [y_C - d_M; y_C + d_M] \tag{13}$$

$$\text{so: } y_I \in Z_a \Rightarrow y_I \in [y_C - d_M; y_C + d_M] \text{ from (12)} \tag{14}$$

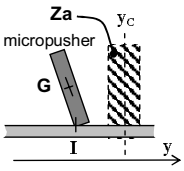

Fig. 9. Definition of approach zone Z_a centered on reference y_C.

Firstly, we consider that the choice between both fine and coarse controllers satisfies:

$$y_I \in Z_a \Rightarrow \text{fine control} \tag{15}$$

$$y_I \notin Z_a \Rightarrow \text{coarse control} \tag{16}$$

Fine control is used to put the micropusher centre of gravity to the reference. We choose to control the position y_G during the fine control.

2) Coarse control: in this section, we analyse the configuration when the contact point I is not in the approach zone Z_a:

$$I \notin Z_a \tag{17}$$

The objective of coarse control is to put contact point I in approach zone Z_a. We therefore generally choose to control position y_I in coarse control. However, the control loop used to control the contact point position I includes the CCD camera which has a sample time of $40\,ms$ (see figure 3). The internal control loop has a sample time of $2\,ms$, defined by the time it takes to read the magnet position, to treat the information and to send the voltage output. Contact point position measurement (by CCD camera) is useful only when the contact point is near the zone Z_a. When point I is far from Z_a, we choose to determine its position by means of a position estimator without the CCD camera. Two cases are possible:

- the contact point is far from the reference position and $(y_I > y_C)$, or
- the contact point is far from the reference position and $(y_I < y_C)$.

In the first case (figure 10(a)), the magnet must be moved to the left. This strategy is noted "left estimator control". In the other case (figure 10(b)), the magnet is moved to the right-hand side, a strategy noted "right estimator control".

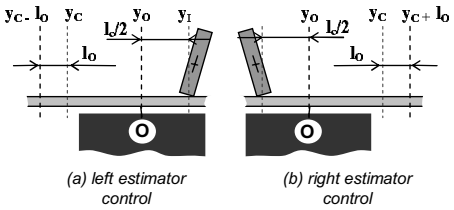

Fig. 10. Configurations when control with contact point position estimator is required.

The two cases are symmetrical, thus we present only the "right estimator control" case $(y_I < y_C)$, in which the contact point I is located to the left of the reference position. The device uses the MACRO movement to move the contact position to the right $(\dot{y}_I > 0)$. Also, orientation d is minimal (table I):

$$d = y_G - y_I = -d_M \tag{18}$$

$$\text{so: } y_I = y_O - \frac{1-K}{K} d_M \quad \text{from (6)} \tag{19}$$

$$= y_O - \frac{(1-K)L_c}{2} \quad \text{from (8)} \tag{20}$$

Distance $(1-K)L_c$ represents the play found in the backlash function. This play depends on the friction properties between the micropusher and the glass slide. We note l_c, an estimation of this play $(1-K)L_c$. Therefore the estimation position $\widetilde{y_I}$ of the position y_I is:

$$\widetilde{y_I} = y_O - \frac{l_c}{2} \quad \text{from (20)} \tag{21}$$

$$\text{with: } l_c \text{ an estimation of distance } (1-K)L_c \tag{22}$$

The estimation $\widetilde{y_I}$ of contact point position y_I is determined only in function of magnet position y_O. If we generalize to both directions (right and left), we obtain:

$$y_I > y_C \Rightarrow \widetilde{y_I} = y_O + \frac{l_c}{2} \tag{23}$$

$$y_I < y_C \Rightarrow \widetilde{y_I} = y_O - \frac{l_c}{2} \tag{24}$$

The switching condition between control with measured position y_I and control with estimated position $\widetilde{y_I}$ depends on

estimated position $\widetilde{y_I}$ and reference position y_C. This condition is defined by parameter l_O:

$$(\widetilde{y_I} - y_C > \frac{l_c}{2} - l_O).(y_I > y_C)$$
$$\Rightarrow \text{left estimator control}$$
$$(\widetilde{y_I} - y_C < -\frac{l_c}{2} + l_O).(y_I < y_C)$$
$$\Rightarrow \text{right estimator control}$$

so:

$$(y_O > y_C - l_O).(y_I > y_C)$$
$$\Rightarrow \text{left estimator control} \quad \text{from (23)}$$
$$(y_O < y_C + l_O).(y_I < y_C)$$
$$\Rightarrow \text{right estimator control} \quad \text{from (24)}$$

Yet, point I is not in zone Z_a, (see equation (17)), so:

$$(y_O > y_C - l_O).(y_I > y_C).(I \notin Z_a)$$
$$\Rightarrow \text{left estimator control} \quad (25)$$
$$(y_O < y_C + l_O).(y_I < y_C).(I \notin Z_a)$$
$$\Rightarrow \text{right estimator control} \quad (26)$$

Parameter l_O defines the transition condition between estimator control and coarse control. The maximal value of l_O is $\frac{l_c}{2}$ (figure 10). With a high value (near $\frac{l_c}{2}$), the major part of the control is performed with estimator control, velocity is high and the risk of overshoot is high too. With a low value (zero or even negative), the major part of the control is performed with coarse control and response time is high. Experimentally, we chose to use l_O as the maximal value of this parameter, which avoids overshoot:

$$l_O = \frac{1}{3} l_c \quad (27)$$

3) Synthesis of control strategy: we have defined three controllers:

- fine controller,
- coarse controller and
- estimator controller (left or right).

According to contact point position y_I, reference y_C and magnet position y_O, the supervisor chooses the controller as described in figure 11.

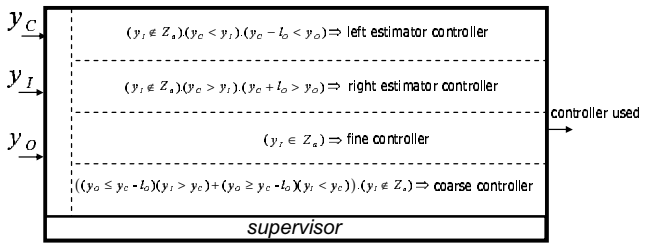

Fig. 11. The supervisor.

B. Three controllers: detailed description

To obtain the coarse/fine control strategy chosen, the supervisor switches between three controllers (fine, coarse and estimator). A description of these three controllers is presented in this section.

1) Fine controller: the objective of fine control is to use a MICRO movement to place the micropusher centre of gravity at reference position y_C (figure 6). We control the position y_G with a standard PI control loop, presented in figure 12, with reference $y_G^C = y_C$.

The controller is adjusted to avoid overshoot. The static gain of the block *PUSHER1D* in MICRO movement is negative, so the controller has a negative gain represented by the block "-1" in the control loop.

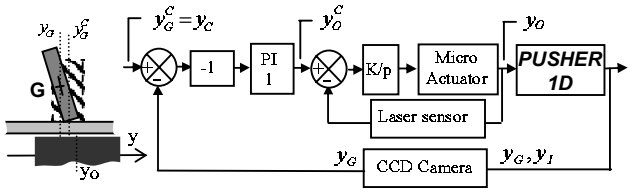

Fig. 12. Fine controller.

2) Coarse controller: the objective of coarse control is to put the contact point I in approach zone Z_a. The position y_I is controlled with the reference $y_I^C = y_C$ (center of Z_a), by means of a standard PI controller defined in figure 13.

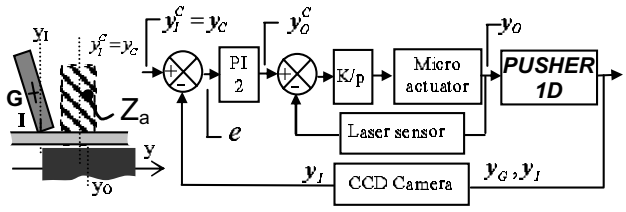

Fig. 13. Coarse controller.

3) Estimator controller: as described previously, there are two cases:

- left estimator control and
- right estimator control.

As previously mentioned, we present only the "right estimator control" case. The estimated position $\widetilde{y_I}$ of the contact point depends on the magnet position y_O measured by the laser sensor:

$$\widetilde{y_I} = y_O - \frac{l_c}{2} \quad \text{from (24)}$$

The control loop built with this estimated contact point position is presented in figure 14.

An equivalent control loop that does not modify the internal loop is presented in figure 15. Using an estimated contact

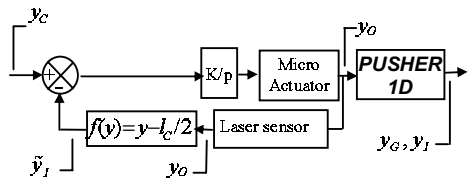

Fig. 14. Right estimator controller.

point position $\widetilde{y_I}$ is equivalent to an open loop control with a reference y_O^C:

$$y_O^C = y_C + \frac{l_c}{2} \tag{28}$$

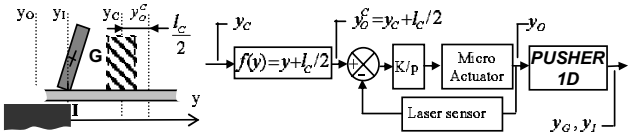

Fig. 15. Right estimator controller: equivalent diagram.

If we generalize to both directions, we obtain:

- right estimator control $\Leftrightarrow y_O^C = y_C + \frac{l_c}{2}$;
- left estimator control $\Leftrightarrow y_O^C = y_C - \frac{l_c}{2}$.

V. Experimental results

Experimental results on the control strategy and micromanipulations performed with the magnetic pusher are described beelow.

A. Control strategy experimentation

In this section, a comparison between the simulated controller and the experimental results is presented.

In figure 16, reference y_C is a square signal ($\pm 80\,\mu m$). We present the simulated and experimental micropusher positions y_G, simulated and experimental magnet positions y_O, and the reference y_C. At $t = 0$, reference position y_C changes:

- first the supervisor uses the right estimator controller to induce a fast movement of the magnet;
- when the position of the magnet satisfies $y_O > y_C + l_O$, the supervisor switches to coarse controller. The change of controllers (at around t=800ms) is not visible in figure 16;
- At $t = 1s$ the pusher is near the reference position, the contact point position enters in the approach zone. The supervisor switches to fine control. The signs of the PI functions of both controllers (coarse and fine) are different, so the controller change induces an about-turn of the magnet. The behaviour of the magnet switches also in MICRO movement (contact point fixed and modification of orientation). The reference position is achieved in fine control.

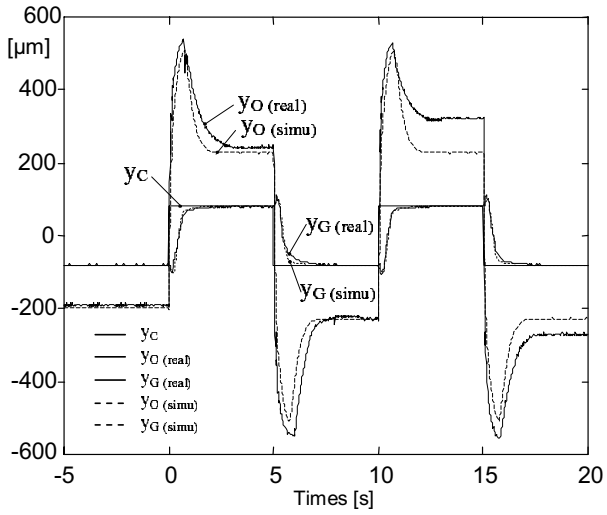

(a) Simulated and experimental positions y_O, y_G and y_C

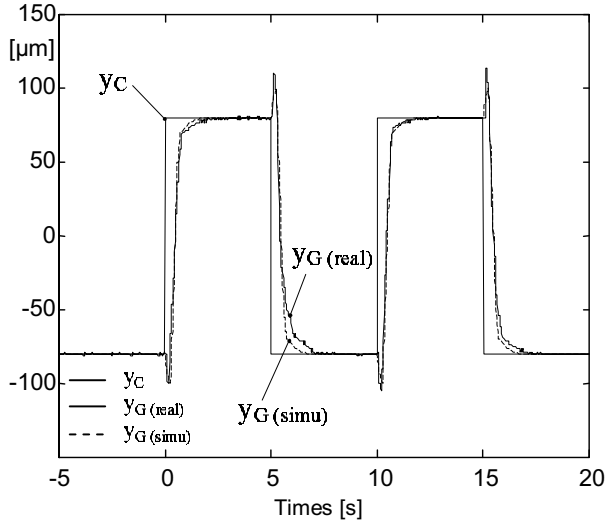

(b) Simulated and experimental positions y_G and y_C

Fig. 16. Simulated and experimental results.

The experimental and simulated results are nearly the same, however some differences are found on the simulated and measured magnet position y_O. In times $0 < t < 5\,s$ and $10 < t < 15\,s$ reference positions y_C and magnet positions are identical while magnet positions y_O are different. For example, at $t = 4\,s$ and $t = 14\,s$, we measure:

$$y_C(t = 4\,s) = y_C(t = 14\,s) = 80\,\mu m \tag{29}$$

$$y_G(t = 4\,s) = y_G(t = 14\,s) = 80\,\mu m \tag{30}$$

$$y_O(t = 4\,s) = 230\,\mu m \neq y_O(t = 14\,s) = 320\,\mu m \tag{31}$$

The experimental device does not have exactly the same behaviour for two identical reference positions. These differences are induced by the sliding properties between the pusher and the glass slide. Actually, these friction properties (static and dynamic friction coefficient) are random functions. The presented simulation does not take into account this random function and uses uniform average sliding properties.

These random sliding conditions explain the differences in magnet positions y_O between $0 < t < 5\,s$ and $10 < t < 15\,s$.

Nevertheless, these random behaviour variations do not disturb the pusher position y_G (figure 16(b)). Consequently, friction behaviour does not disturb the objective of our controller.

In a standard controller which does not use the MICRO movement to achieve the reference, the precision is disturbed by the stick-slip effect. Yet, stick slip pusher jumps depend on the surface properties and range from 5 to 20 micrometers [10]. Thus, repeatability of standard controllers is greatly limited by this physical constraint. With our proposed controller, the reference is achieved in MICRO movement without stick-slip disturbances. Consequently, experimental repeatability is limited only by the CCD camera resolution ($1\,\mu m$). This repeatability is sufficient to manipulate single biological cells such as oocytes.

At the present time, no theoretical stability study is under way, but the stability of this controller was tested successfully by simulation and experimental tests. Naturally, friction conditions are not uniform on the surface and the noise does not disturb the controller. Moreover, simulations of noise on model parameters (L_c and stick slip jumps value) proved the stability of our controller.

B. Micromanipulations

Polystyrene balls 50 μm in diameter were micromanipulated with the One Degree of Freedom (DOF) device whose control strategy is described in this article. Open loop micromanipulations of immature human oocytes of about 150 μm in diameter were made with a new 2-DOF magnetic micropusher. The principle used is the same as in the 1-DOF device. A nickel ferromagnetic pusher follows the planar movement of a magnet. The 2-DOF magnet is a cylindrical magnet with axis z to obtain the same behaviour in both planar DOF x and y.

An example of a 2-DOF open loop oocyte micromanipulation is presented in figure 17. This video was made without white paper under the glass slide so as to render visible both the micropusher and the magnet. To obtain a better view of oocyte and pusher, white paper must be placed under the glass slide and a specific lighting is necessary. In pictures 1 and 2, the magnet movement direction is $y+$ and the pusher follows the magnet in the y direction. In pictures 3, 4 and 5, magnet movement direction is $x+$ and the pusher trajectory is a coupled movement in x and y directions. In picture 6, the magnet moves a half turn in the x direction to release the oocyte.

VI. Conclusion

The microdevice presented in this article makes it possible to push oocytes in a droplet of biological liquid on a glass slide. In this device, the micropusher is a ferromagnetic object that follows the movement of a permanent magnet located under the glass slide. A movement of the contact point between the micropusher and the glass slide induces a macro movement of the pushed object, while a rotation of the micropusher induces a micro movement of the object. Thus, the micropusher is comparable to a particular micro-macro positioning system, where both micro and macro movements depend on the magnet position controlled by a computer. This micro-macro positioning system, which has only one input (the magnet position), cannot be controlled by usual micro-macro control strategies. Consequently, we propose a specific coarse-fine control strategy based on three basic PI controllers specialized in each elementary step (approach, coarse positioning, and fine positioning). A supervisor switches between these specialized controllers depending on the state of the device (position and orientation of the pusher and magnet position). This specific control strategy makes possible a precision of one micrometer within a wide range, despite stick-slip disturbances.

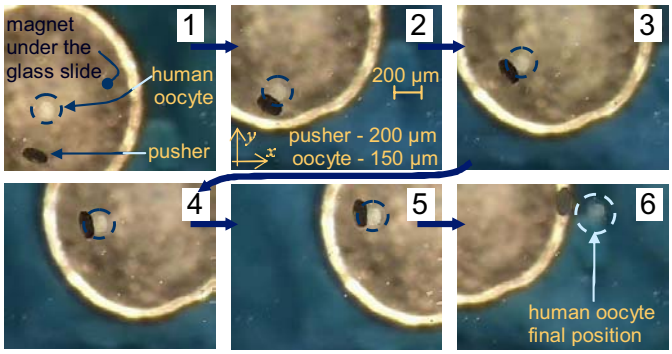

Fig. 17. 2-DOF open loop manipulation of an Oocyte ($150\,\mu m$).

Acknowledgements

This research was supported by the LAB (Laboratory of Automation - Besançon - CNRS - UFC - ENSMM - France: http://www.lab.cnrs.fr). The authors thank Prof. Roux (Genetic and reproduction research group of the University of Franche-Comté, Besançon, France) for his collaboration on oocyte micromanipulations.

References

[1] F. Arai, H. Maruyama, T. Sakami, A. Ichikawa, and T. Fukuda. Pinpoint injection of microtools for minimally invasive micromanipulation of microbe by laser trap. *IEEE/ASME Trans. on Mechatronics*, 8(1):3–9, 2003.

[2] M. Frenea, S. P. Faure, B. Le Pioufle, Ph. Coquet, and H. Fujita. Positioning living cells on a high-density electrode array by negative dielectrophoresis. *Materials Science and Engineering*, 23:597–603, 2003.

[3] D-H Kim, B. Kim, S. Yun, and S. Know. Cellular force measurement for force reflected biomanipulation. In *Proceedings of the 2004 IEEE ICRA*, pages 2412–17, New Orleans, USA, April 2004.

[4] G. Li, Ning Xi, M. Yu, F. Salem, D. H. Wang, and J. Li. Manipulation of living cells by atomic force microscopy. In *Proceedings of the 2003 IEEE/ASME International Conference on Advanced Intelligent Mechatronics (AIM 2003)*, pages 862–67, Port Island, Kobe, Japan, July 2003.

[5] Y. Sun and B. J. Nelson. Mems for cellular force measurements and molecular detection. *Journal of Information Acquisition (IJIA)*, 1:23–32, 2004.

[6] Y. Sun, K. T. Wan, B. J.Nelson, J. Bischof, and K. Roberts. Mechanical property characterization of the mouse zona pellucida. *IEEE Transactions on NanoBioScience*, 2(4):279–286, 2003.

[7] M. Boukallel, J. Abadie, and E. Piat. Levitated micro-nano force sensor using diamagnetic materials. In *Proc. Of the Int. Conference on Robotics and Automation*, Taipei, Taiwan, May 2003.

[8] M. Boukallel, M. Gauthier, E. Piat, J. Abadie, and C. Roux. Microrobots for in vitro fertilization applications. *Cellular and Molecular biology*, 50(3):267–74, 2004.

[9] M. Gauthier and E. Piat. Microfabrication and scale effect studies for a magnetic micromanipulation system. In *Proc. of the IEEE International Conference on Intelligent Robots and Systems - IROS02*, volume 2, pages 1754–59, Lausanne - Switzerland, 30 sept - 4 Oct 2002.

[10] M. Gauthier and E. Piat. An electromagnetic micromanipulation system for single cell manipulation. *Journal of Micromechatronics*, 2(2):87–119, Feb 2004.

[11] B. Bae, N. Kim, H. Kee, S.-H. Kim, Y. L., S. Lee, and K. Park. Feasibility test of an electromagnetically driven valve actuator for glaucoma treatment. *Journal of Microelectromechanical Systems*, 11(4):344–54, august 2002.

[12] T. Bourouina, E. Lebrasseur, G. Reyne, A. Debray, H. Fujita, A. Ludwig, E. Quandt, H. Muro, T. Oki, and A. Asaoka. Integration of two degree-of-freedom magnetostrictive actuation and piezoresistive detection: application to a two-dimensional optical scanner. *Journal of Microelectromechanical Systems*, 11(4):355–61, august 2002.

[13] O. Cugat, J. Delamare, and G. Reyne. Magnetic micro-actuators and systems (magmas). *IEEE Transactions on Magnetics*, 39(6):3607–12, nov. 2003.

[14] H. Guckel. Progress in magnetic microactuators. *Microsystem technologies.*, 5(2):59–64, 1998.

[15] S. Guo, Y. Sasaki, and T. Fukuda. A new kind of microrobot in pipe using driving fin. In *Proceedings of the 2003 IEEE/ASME International Conference on Advanced Intelligent Mechatronics (AIM 2003)*, pages 697–702, Port Island, Kobe, Japan, July 2003.

[16] Anson Hatch, Andrew Evan Kamholz, Gary Holman, Paul Yager, and Karl F. Böhringer. A ferrofluidic magnetic micropump. *Journal of Microelectromechanical Systems*, 10(2):215–221, June 2001.

[17] L. K. Lagorce, O. Brand, and M.G. Allen. Magnetic microatuator based on polymer magnets. *Journal of micromechanical systems*, 8(1):3–14, 1999.

[18] Chang Liu and Yi Y. W. Micromachined magnetic actuators using electroplated permalloy. *IEEE transactions on magnetics*, 35(3):1976–85, 1999.

[19] J Y Park and M G Allen. Development of magnetic materials and processing techniques applicable to integrated micromagnetic devices. *Journal of Micromechanics and Microengineering*, 8(4):307–316, 1998.

[20] K. B. Yesin, K. Vollmers, and B. J. Nelson. Analysis and design of wireless magnetically guided microrobots in body fluids. In *Proceedings of the 2004 IEEE ICRA*, pages 1333–38, New Orleans, USA, April 2004.

[21] R. Feynman. Infinitesimal machinery. *J. of Microelectromechanical System*, 2(1), 1993.

[22] M. Gauthier and E. Piat. Force study applied by a planar micromanipulator to biological objects. *Journal Européen des Systèmes Automatisés*, 36(9):1249–64, december 2002.

[23] W. Yim and S. N. Singh. Nonlinear inverse and predictive end point trajectory control of flexible macro-micro manipulators. *Transactions of the ASME journbal of Dynamics Systems, Measurement and Control*, 119:412–420, 1997.